Received: 10 July 2018 | Accepted: 7 December 2018

DOI: 10.1111/jmg.12467

ORIGINAL ARTICLE

WILEY Journal of METAMORPHIC GEOLOGY

The partial equilibration of garnet porphyroblasts in pelitic schists and its control on prograde metamorphism, Glen Roy, Scotland

Tim J. Dempster | **Mairi I. Gilmour** | **Peter Chung**

School of Geographical & Earth Sciences, University of Glasgow, Glasgow, UK

Correspondence
Tim J. Dempster, School of Geographical and Earth Sciences, University of Glasgow, Glasgow, UK.
Email: tim.dempster@glasgow.ac.uk

Handling Editor: Donna Whitney

Abstract

Garnet porphyroblasts in sillimanite-bearing pelitic schists contain complex textural and compositional zoning, with considerable variation both within and between adjacent samples. The sillimanite-bearing schists locally occur in regional Barrovian garnet zone assemblages and are indicative of a persistent lack of equilibrium during prograde metamorphism. Garnet in these Dalradian rocks from the Scottish Highlands preserves evidence of a range of metamorphic responses including initial growth and patchy coupled dissolution–reprecipitation followed by partial dissolution. Individual porphyroblasts each have a unique and variable response to prograde metamorphism and garnet with mainly flat compositional profiles co-exists with those containing largely unmodified characteristic bell-shaped Mn profiles. This highlights the need for caution in applying traditional interpretations of effective volume diffusion eliminating compositional variation. Cloudy garnet with abundant fluid inclusions is produced during incomplete modification of the initial porphyroblasts and these porous garnet are then particularly prone to partial replacement in sillimanite-producing reactions. The modification of garnet via a dissolution–reprecipitation process releases Ca into the effective whole-rock composition, displacing the pressure–temperature positions of subsequent isograd reactions. This represents the first report of internal metasomatism controlling reaction pathways. The behaviour of garnet highlights the importance of kinetic factors, especially deformation and fluids, in controlling reaction progress and how the resulting variability influences subsequent prograde history. The lack of a consistent metamorphic response, within and between adjacent schists, suggests that on both local and regional scales these rocks have largely not equilibrated at peak metamorphic conditions.

KEYWORDS

coupled dissolution–reprecipitation, garnet zoning, internal metasomatism, reaction controls, sillimanite isograd

1 | INTRODUCTION

Garnet is probably the most widely studied mineral in regional metamorphic rocks (e.g. Bell & Johnson, 1989; Caddick, Konopásek, & Thompson, 2010; Carlson, Hixon, Garber, & Bodnar, 2015; Spear, 1993; Yang & Rivers, 2001). In low and medium grade conditions, volume diffusion of the divalent cations is ineffective at the scale of typical porphyroblasts (Carlson, 2006; Kohn, 2014) and hence garnet is capable of recording changing compositions during growth (Holdaway, 2001; Spear, Kohn, Florence, & Menard, 1990; Thompson, Tracy, Lyttle, & Thompson, 1977; Tracy, Robinson, & Thompson, 1976). As such, it may preserve a record of the evolution of conditions and a range of thermobarometry techniques are largely based on analyses of garnet zoning profiles (e.g. Moynihan & Pattison, 2013). At higher grades, progressive flattening of garnet compositional profiles has been reported and this is typically interpreted to be due to progressively more effective volume diffusion at these elevated temperatures (Dempster, 1985; Mueller, Watson, & Harrison, 2010; Yardley, 1977a). Such profiles in combination with experimental constraints on the rates of cation diffusion in garnet (Borinski, Hoppe, Chakraborty, Ganguly, & Bhowmik, 2012; Carlson, 2006; Ganguly, 2010) have led to a growing literature documenting applications of geospeedometry, whereby time-scales of metamorphic events are estimated (Ague & Baxter, 2007; Caddick et al., 2010; Chu & Ague, 2015; Lasaga, 1983; Mueller et al., 2010; Spear, 2014; Viete, Hermann, Lister, & Stenhouse, 2011). Thus, garnet compositions are typically interpreted as recording growth zoning at lower temperatures and progressive diffusional modification at higher temperature.

Garnet porphyroblast compositions may also be reset by coupled dissolution–reprecipitation mechanisms (Ague & Axler, 2016; Dempster, La Piazza, Taylor, Beaudoin, & Chung, 2017; Martin et al., 2011; Pollok, Lloyd, Austrheim, & Putnis, 2008), although the effectiveness of such processes relative to the size and abundance of typical garnet is uncertain. However, because of the wide range of possible responses to changing conditions, garnet within mid-amphibolite facies conditions offers the opportunity to investigate the kinetic controls on metamorphic reactions. Consequently, it is capable of partially preserving both the textural and chemical evidence of reaction progress that would be lost in the vast majority of coexisting metamorphic minerals.

In this study, we investigate the variable response of garnet to a sillimanite-producing reaction during Barrovian metamorphism of garnet mica schists from the Scottish Highlands (Barrow, 1893). The different responses of garnet to changing *P–T* conditions raise fundamental questions concerning the concept of progressive metamorphism (Carlson, Hixon, Garber, & Bodnar, 2015; Pattison & Tinkham, 2009; Waters & Lovegrove, 2002), and the interpretation of compositional zoning profiles in garnet. This is consistent with other investigations that suggest that metamorphic reactions may not occur on a macroscopic scale if low rates of intergranular and volume diffusion persist, and limited fluids are available to enhance transport rates (Carlson, Pattison, & Caddick, 2015; Dempster, Symon, & Chung, 2017).

2 | GEOLOGICAL BACKGROUND AND PETROGRAPHY

The Leven schists in Glen Roy, Scotland, represent part of a Neoproterozoic sedimentary sequence within the Appin Group of the Dalradian Supergroup (Harris, Haselock, Kennedy, & Mendum, 1994; Phillips et al., 1994). These garnet mica schists have been reported as occupying an extensive Barrovian garnet zone with rare staurolite, with estimated peak amphibolite facies conditions at 500–600°C, 0.7–0.8 GPa (Phillips et al., 1994; Richardson & Powell, 1976). No strong metamorphic field gradients have been reported from this area, although Dempster, La Piazza, et al. (2017) highlighted local kinetic controls on the limited introduction of staurolite in the Leven Schists 8 km to the southwest. The age of regional metamorphism in these rocks is uncertain, as polymetamorphism is commonly reported in the Dalradian schists (Dempster & Harte, 1986; Dempster & Jess, 2015; Dempster et al., 2002).

This study focuses on two immediately adjacent samples (ugr0 and ugr1) from the northern side of upper Glen Roy (UK Ordnance Survey Grid Ref NN3671 9239), northeast of Brae Roy Lodge. Both samples contain relatively large (2–4 mm) euhedral to subhedral garnet porphyroblasts within a schistose fabric, dominated by fine-grained micaceous (~50–120 μm) units interbedded with thin (1–2 mm) quartzofeldspathic layers (Figure 1). There is no obvious textural difference between the two samples and both samples are dominated by ~40% muscovite with a similar amount of quartz and plagioclase combined. No veins are observed close to the samples in the field. Mineral assemblages are identical in each sample. Fibrous sillimanite and staurolite are present in both, although much more abundant (1.6 and 2.1% respectively) in ugr0 than ugr1, where they are present in trace amounts ≤0.1% (Table 1). Both of these phases are preferentially located within the cleavage domain close to the edge of the garnet porphyroblasts (Figures 1b and 2). Staurolite is subhedral up to 1 mm in ugr0 and may display limited partial retrograde alteration along cracks. Within ugr1, it forms rare very small (50–100 μm) equant grains. Biotite forms a porphyroblastic phase (up to 3 mm) and a fabric-forming element within both rocks (Figure 1). Neither sample contains

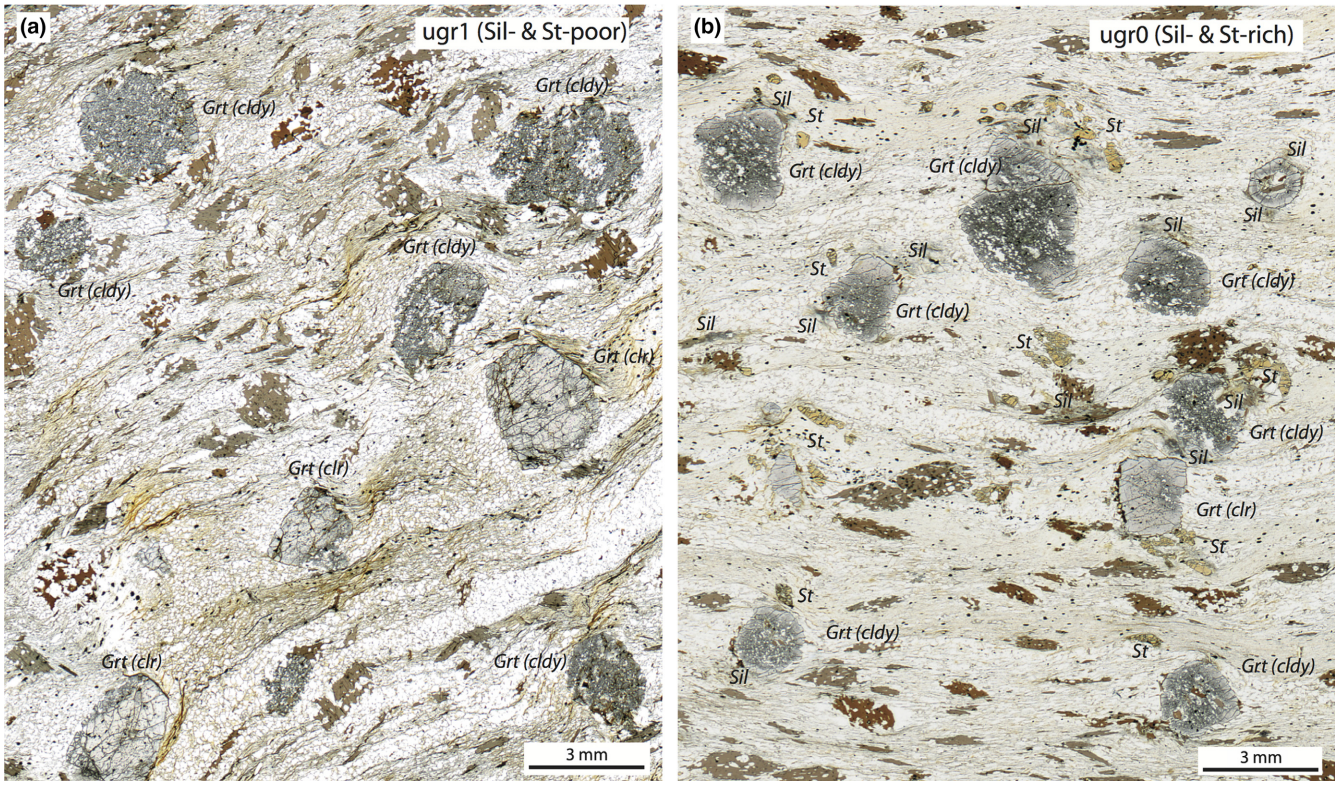

FIGURE 1 Thin section photomicrographs of (a) sample ugr1 and (b) sample ugr0. Positions of largest staurolite (St) and sillimanite (Sil) clusters are shown around some of the larger garnet porphyroblasts. Large garnet porphyroblasts are labelled according to whether they are dominantly 'cloudy' (Grt cldy) or 'clear' (Grt clr). Mineral abbreviations follow Whitney and Evans (2010) [Colour figure can be viewed at wileyonlinelibrary.com]

much evidence of retrogression, with trace amounts of retrograde chlorite (0.5%) after both garnet and biotite. Plagioclase typically shows a dusty alteration.

Garnet porphyroblasts are texturally extremely variable in both samples (Figure 3). Three main types of garnet are present: clear garnet with small mineral inclusions (Figure 3a); cloudy garnet (Figure 3b–d); and, clear inclusion-free rims (Figure 3c,d). Individual porphyroblasts may be dominated by either clear or cloudy garnet, but typically a mixture of types is present in many porphyroblasts (Table 1). Clear inclusion-free rims are most commonly associated with cloudy garnet in the sillimanite-rich assemblage in ugr0 (Figure 3c).

Clear garnet may dominate some individual porphyroblasts, especially in sample ugr1 (Figure 1a). It is characterized by either no inclusions or sparse (<10%), small (10–20 μm), equant quartz and Fe-oxide inclusions (Figures 3a and 4a). Garnet with high proportions of such types is typically well-shaped with relatively planer margins (Figures 1 and 3a). However, all such garnet contains some cloudy areas. The mineral inclusions in these clear areas of the porphyroblasts may display a weak planer alignment at an angle to the external muscovite-dominated fabric.

Many porphyroblasts or parts of porphyroblasts are dominated by dark cloudy garnet with abundant tiny fluid inclusions (Figure 3b,c,e). Such inclusions typically show crystallographic alignment (Figure 3e), although where the inclusions are very abundant the alignment may be more difficult to discern. The areas of cloudy garnet are associated with abundant large (100–200 μm) irregular-shaped inclusions of quartz (Figure 3e,g). Cloudy garnet is slightly more abundant within the sillimanite-poor sample (ugr1), forming on average 40% of each porphyroblast in comparison to 37% of the garnet in the sillimanite-rich sample ugr0 (Table 1). It may form >80% of the garnet in some individual porphyroblasts (Table 1). Cloudy garnet has a greater proportion of inclusions than the equivalent clear porphyroblasts (Figure 4a). Typically porphyroblasts dominated by cloudy garnet have a slightly more rounded shape with irregular inclusion-rich margins (Figure 1). Some porphyroblasts have elongate clear and cloudy domains that are roughly aligned with the external micaceous fabric (Figure 3a). In others, the distribution of these two types is patchy (Figure 3b,d). Most commonly, cloudy garnet dominates the core areas of the porphyroblast (Figure 3c), but rims of cloudy garnet around a clear core are also observed. The contact between these two garnet types is typically transitional and marked by areas of the porphyroblasts with a weak 'cloudy' texture, and a low density of fluid inclusions,

TABLE 1 Modal mineralogy of the two samples investigated and proportions of garnet and inclusion types within the largest 15 porphyroblasts from each sample. Mineral abbreviations follow Whitney and Evans (2010). Garnet types based on point counting the 15 largest porphyroblasts in each thin section, include: clear - original relatively inclusion poor; rim – inclusion-free rim at porphyroblast edge or around inclusion; cloudy – dark garnet with abundant aligned fluid inclusions; ambig – ambiguous, transitional between clear and cloudy with a scattering of non-aligned small fluid inclusions. Inclusion types: small – equant, small mineral inclusions; Sil – sillimanite-bearing inclusions; irreg – irregular-shaped typically large mineral inclusions (Sil-free)

	Ms	Qz	Pl	Bt	Grt	St	Sil	Opq	Chl	Rt
ugr0	39.3	23	12	11.9	8.6	2.1	1.6	0.7	0.5	0.2
ugr1	40	27.8	12.2	14.1	4.4	trace	0.1	0.7	0.5	–

	grt type				Inclusion type		
Porph no	**Clear**	**Rim**	**Cloudy**	**Ambig**	**Small**	**Sil**	**Irreg**
ugr0							
1	13	19	35	10	3	11	10
2	3	32	42	4	0	13	10
3	1	30	35	5	0	17	12
4	17	29	27	6	10	7	4
5	31	15	22	11	8	3	11
6	21	24	23	12	15	1	4
7	1	30	39	2	3	10	15
8	0	38	41	0	1	8	12
9	0	34	38	2	0	21	6
10	3	30	37	4	0	15	11
11	17	26	33	4	7	8	5
12	10	28	43	6	6	3	5
13	0	26	50	0	0	17	7
14	0	30	36	11	0	14	9
15	0	24	50	2	0	6	17
Mean	8	28	37	5	4	10	9
ugr1							
1	35	6	34	13	9	0	8
2	15	12	38	10	3	7	16
3	0	11	45	4	1	11	29
4	63	6	20	3	5	2	2
5	53	6	25	1	6	1	9
6	24	14	43	3	2	5	10
7	21	14	38	2	9	4	12
8	19	14	33	10	11	6	8
9	0	14	60	0	0	16	10
10	38	13	30	2	4	9	4
11	15	12	43	2	2	12	15
12	0	14	57	0	0	20	9
13	73	3	20	0	3	2	3
14	0	20	60	0	1	12	7
15	4	14	57	1	0	13	14
Mean	24	12	40	3	4	8	10

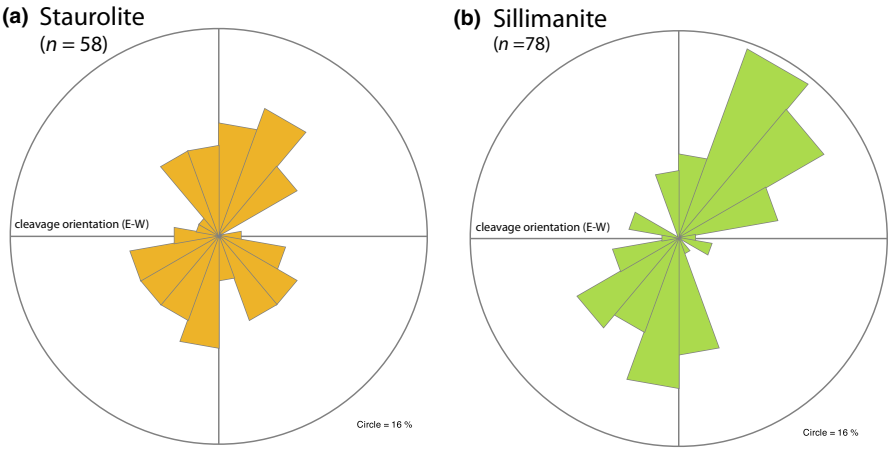

FIGURE 2 Rose diagrams showing the angular relationship between the locations of (a) staurolite; and, (b) large sillimanite clusters and mats, and the alignment of the muscovite fabric (E–W) measured relative to the centre of each garnet porphyroblast (sample urg0) [Colour figure can be viewed at wileyonlinelibrary.com]

listed as 'ambiguous' in Table 1. In other instances, these transitions may be sharply defined (Figure 3d).

Clear inclusion-free rims of garnet form at the edge of most areas of cloudy garnet, either at junctions with the matrix or adjacent to silicate inclusions (Figure 3c,f,g). Such zones are of variable width (typically a few microns to a few hundred microns; Figure 4b) but particularly prominent around the irregular sillimanite-bearing inclusions or matrix (Figure 3f,h). The clear rims are much less prominent and less abundant in sample ugr1, forming ~12% of the overall garnet population in comparison to 28% in the sillimanite-rich sample (ugr0) (Table 1). Due to their contrasting textural characteristics, rims are much more obvious when adjacent to cloudy garnet (Figure 3f). Such transitions between garnet types are often sharply defined but may also be associated with a gradual change in the abundance of fluid inclusions over a few hundred microns (Figure 3f). The geometry of the rim-cloudy garnet transition is locally influenced by fractures within the garnet with the clear areas extending into cloudy areas symmetrically either side of the fracture (Figure 3h). In the more sillimanite-rich sample (ugr0), some atoll-like garnet is present, with coarse multiphase inclusions of quartz–sillimanite–biotite occupying much of the centre of the porphyroblast (Figure 3j). These garnet are dominated by a combination of cloudy garnet and extensive clear rims both at the margins of the porphyroblast and adjacent to the sillimanite-bearing inclusions and embayments (Figure 3j). Garnet typically has quartz-rich, muscovite-poor pressure shadows (Figure 1) and adjacent to these areas the garnet lacks clear rims and the matrix lacks sillimanite (Figure 2b).

Within sample ugr1, immediately adjacent porphyroblasts are dominated by either cloudy garnet with no clear patches, or clear garnet with small quartz inclusions with very few areas of cloudy garnet (Figure 1a). In such instances, the porphyroblasts dominated by cloudy garnet occur in areas of the sample with more abundant biotite porphyroblasts (Figure 1a) with ~5–20% more biotite in the layers dominated by a higher proportion of cloudy garnet (Figure 4c).

All garnet porphyroblasts have adjacent sillimanite, but the amount of the latter is very variable, ranging from individual isolated needles associated with largely clear porphyroblasts in ugr1 to extensive mats of fibrolite associated with the atoll-like garnet and the edges of porphyroblasts in ugr0 (Figure 3h). Sillimanite is an order of magnitude more abundant in ugr0 (Table 1) and is typically concentrated in larger irregular-shaped inclusions within generally cloudy areas of the garnet or within large embayments at the margins of the porphyroblasts (Figure 3f). Both sillimanite and staurolite are strongly concentrated in areas where the edges of garnet porphyroblasts impinge on the muscovite-rich fabric away from pressure shadow areas (Figure 2). Where present in relatively small quantities, sillimanite is strongly associated with quartz, with individual fibrolite needles encased within quartz either within the general matrix or where the quartz occurs as inclusions within garnet (Figure 3g). The more abundant the sillimanite, the wider the clear rim in the adjacent garnet (Figure 4b). Clear rims are particularly wide next to sillimanite at the margins of the porphyroblast in comparison to those adjacent to sillimanite-bearing inclusions (Figures 3c,h and 4b). The extent of the clear garnet rim that develops is also unique to the individual garnet porphyroblast (Figure 4b). Sillimanite may be present within the small quartz inclusions in the areas of clear garnet. Such occurrences are rare and typically restricted to a single fibrolite needle. These sillimanite-bearing inclusions appear to be located close to some of the larger fractures that cross-cut the garnet.

3 | METHODS

Large (7 × 5 cm) polished thin sections of the two samples were cut perpendicular to foliation. Textural characterization of garnet was based on a combination of the

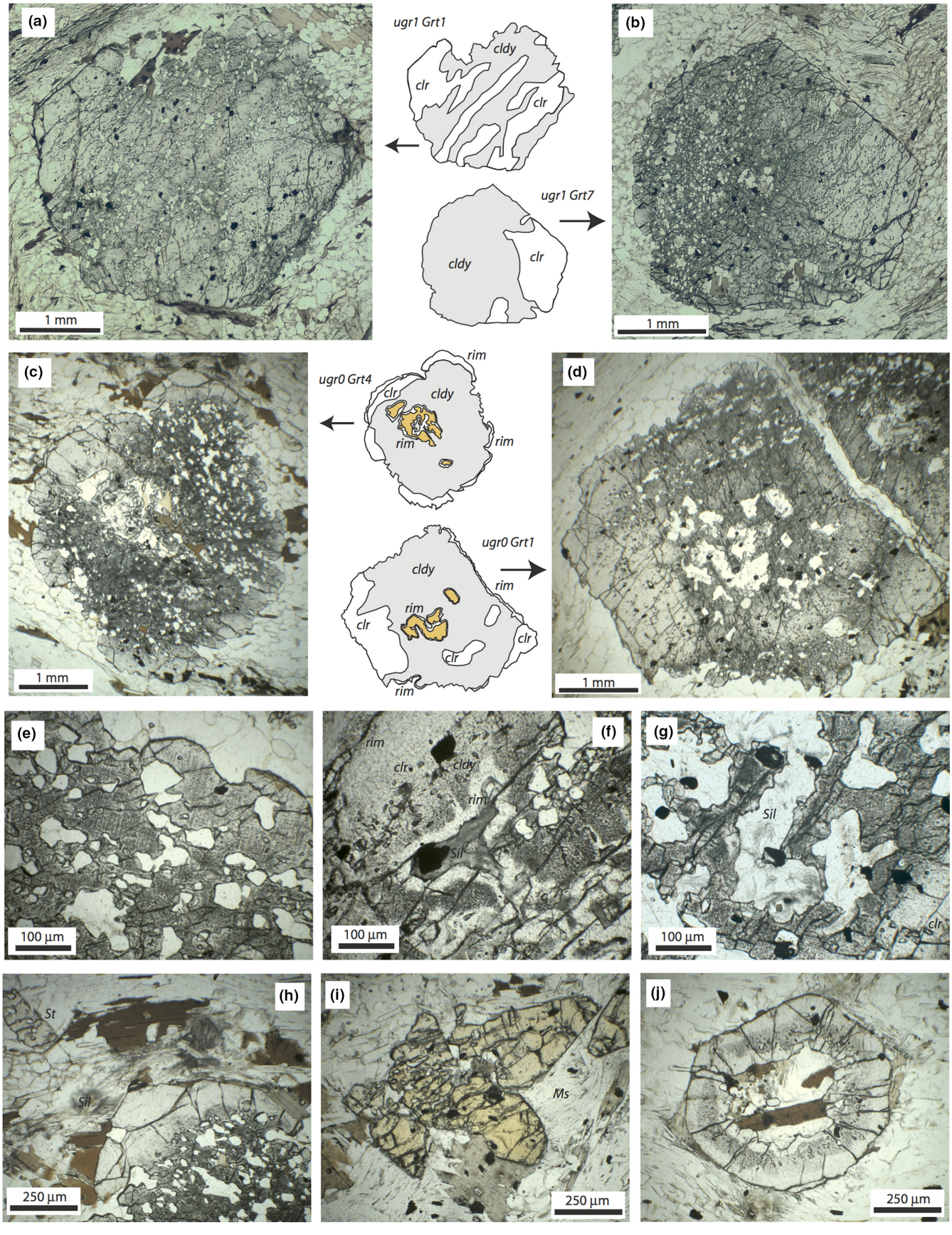
(a)
1 mm
ugr1 Grt1
cldy
clr
clr
ugr1 Grt7
cldy
clr
(b)
1 mm
(c)
1 mm
ugr0 Grt4
rim
clr
cldy
rim
rim
ugr0 Grt1
cldy
rim
rim
clr
clr
clr
rim
(d)
1 mm
(e)
100 µm
(f)
rim
clr
cldy
rim
Sil
100 µm
(g)
Sil
clr
100 µm
(h)
St
Sil
250 µm
(i)
Ms
250 µm
(j)
250 µm

FIGURE 3 Various porphyroblast textures in plane polarized light. (a–d) Large garnet porphyroblasts with adjacent cartoons summarizing their internal textures (cldy – cloudy [shaded]; clr – clear; rim – inclusion-free rim; yellow areas – sillimanite-bearing inclusions). (a) Porphyroblast (ugr1 Grt1) with areas of dark cloudy texture and remnants of clear garnet showing approximate alignment with the micaceous external fabric. (b) Porphyroblast (ugr1 Grt7) with extensive replacement by inclusion-rich cloudy garnet. (c) Porphyroblast (ugr0 Grt4) with cloudy inclusion-rich interior, large irregular sillimanite-bearing inclusions, clear rims adjacent to these inclusions and along some margins. (d) Porphyroblast with both clear and cloudy areas (ugr0 Grt1), narrow clear rims adjacent to sillimanite inclusions and some margin. (e) Irregular-shaped quartz inclusions and alignment of fluid inclusions within cloudy garnet (ugr0 Grt5). (f) Irregular-shaped sillimanite-rich inclusions (sil) with clear rims (rim) in the adjacent garnet. Porphyroblast has an outer clear rim (rim) (ugr0 c4), with an inner zone of minor fluid inclusions and small mineral inclusions (clr) then a zone of cloudy garnet (cldy). (g) Cloudy garnet with irregular-shaped quartz and plagioclase inclusions, with needles of sillimanite enclosed within quartz (ugr0 Grt1). Thin rims of clear garnet are present adjacent to the sillimanite-bearing inclusions. Patch of clear garnet (clr) with small quartz inclusions present in lower right of image. (h) Wide clear rim of inclusion-free garnet adjacent to mat of matrix sillimanite (Sil), next to core of cloudy garnet with abundant irregular-shaped quartz inclusions (ugr0 Grt2). Fractures in the garnet rim locally influence to the shape of the cloudy-clear rim boundary (centre of image). Well-shaped staurolite (St) is adjacent to the matrix sillimanite (Sil). (i) Euhedral staurolite porphyroblasts (ugr0) adjacent to aligned muscovite (Ms). (j) Atoll garnet (ugr0 Grt16) with outer and inner clear rims and an intermediate rim of cloudy garnet. Central core has an aggregate of biotite, quartz and sillimanite [Colour figure can be viewed at wileyonlinelibrary.com]

abundance of fluid inclusions, size, shape and alignment of mineral inclusions. Although a somewhat subjective classification, only a small proportion of garnet is of uncertain type and 'ambiguous' (Table 1). Following the methods described in Dempster, La Piazza, et al. (2017), X-ray maps and compositional traverses were generated using a Carl-Zeiss Sigma VP electron microscope operated at 20 kV, with Oxford Instruments X-Max 80 energy dispersive spectrometry typically with 2 μm spacing between points. Major element zoning profiles were processed using AZTEC Software 3.0. Modal mineralogy of each sample and proportions of different textural types of garnet were determined through point counting, the latter based on the analysis of the 15 largest garnet porphyroblasts in each thin section. Local variations in modal percentages of matrix biotite were assessed by using 'ImageJ' software, comparing restricted areas within approximately one radius distance of the edge of each large garnet porphyroblast.

4 | RESULTS – GARNET CHARACTERISTICS

4.1 | Clear garnet with small inclusions

Clear garnet forms ~24% of the garnet porphyroblasts in ugr1 but an average of 8% in ugr0 (Table 1). Typically, those porphyroblasts dominated by clear garnet have zoning profiles most similar to the general Mn-rich bell-shaped profiles (Figure 5a,b) that are very commonly reported from lower amphibolite facies pelitic schists (Atherton, 1968; Harte & Henley, 1966; Hollister, 1966). Mn contents of 12 mol.% spessartine are present in the core areas with ~1–2 mol.% at the porphyroblast rims (Figure 5). The Ca distribution is typically somewhat variable due to the presence of zones of cloudy garnet, but core areas of the largest clear garnet porphyroblasts contain up to 18–19 mol.% grossular, with a steady decrease

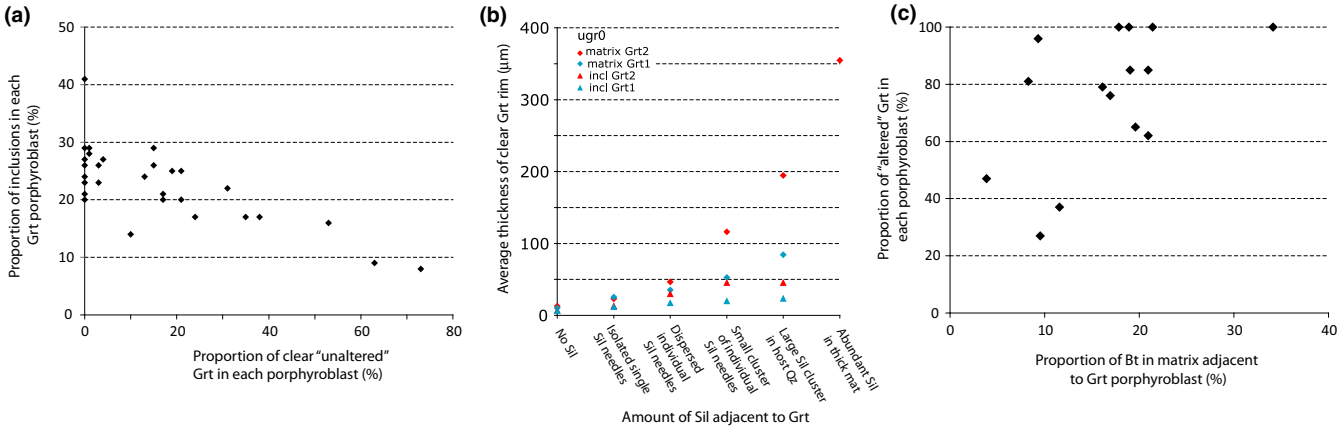

FIGURE 4 (a) Plot of total inclusions in each individual garnet porphyroblast against the % of clear garnet in that porphyroblast. (b) Plot showing average width of clear rims of garnet as a function of the abundance sillimanite in the immediately adjacent matrix and inclusion. (c) Plot showing percentage of biotite in the matrix adjacent to garnet porphyroblasts as a function of the proportion of altered non-'clear' garnet in that individual porphyroblast (ugr1) [Colour figure can be viewed at wileyonlinelibrary.com]

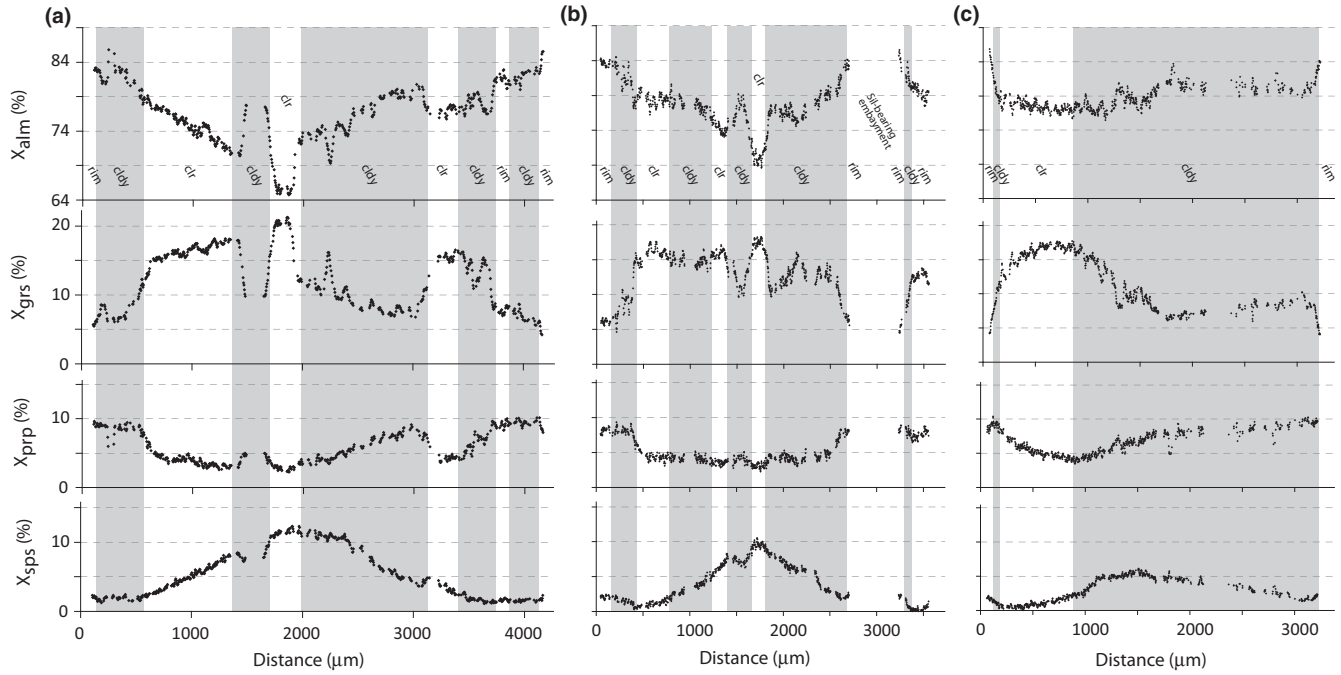

FIGURE 5 Compositional zoning profiles of dominantly clear (clr) garnet with cloudy (cldy) zones and thin clear rims (rim). (a) ugr1 c1; (b) ugr1 Grt 1; (c) ugr1 Grt7

to ~13 mol.% towards the porphyroblast edge (Figure 5c). $X_{M/FM}$ typically shows a gradual increase from the core towards the rim (4–10%) within the clear garnet areas. Plagioclase inclusions within the clear garnet are rare, and within the central areas have relatively Na-rich compositions.

4.2 | Cloudy garnet with large irregular inclusions

Porphyroblasts dominated by cloudy garnet are characterized by relatively flat compositional zoning profiles (Figure 6) in comparison to the clear garnet porphyroblasts (Figure 5). Low amplitude Mn cores are present, with up to ~4 mol.% spessartine (Figure 6a), although Mn profiles are typically flat (Figure 6c), especially within ugr0 and may show a slight enrichment in Mn towards the outer rim (Figure 6). In porphyroblasts where cloudy garnet dominates the core areas, Ca contents are relatively uniform (5–6 mol.% grossular), in comparison to the noisy profiles of the other end-member compositions (Figure 6a). Plagioclase inclusions within the cloudy garnet have variable compositions ranging from andesine to albite without following any obvious spatial distribution, although the majority of inclusions in cloudy garnet are typically oligoclase (~An_{25}). The latter are also representative of plagioclase in the matrix although those in the matrix typically include some more sodic compositions (down to An_{15}).

Where domains or zones of cloudy garnet cut across clear garnet very variable compositional zoning is present (Figure 5a,b). The former having relatively low Ca, high Mg and Fe and high M/FM compositions, broadly similar to the rim compositions of the clear garnet but with significantly lower Ca contents. Cloudy garnet lacks a consistent composition when within a dominantly clear garnet porphyroblast. In core areas of cloudy garnet, Mn contents are typically lower than the host clear garnet, but if the cloudy areas are located towards the outer portion of the porphyroblast, the cloudy areas are typically slightly enriched in Mn relative to the clear garnet. Rim compositions of porphyroblasts may be variable depending on whether edges are locally composed of clear or cloudy garnet (Figure 5b). The transitions between clear and cloudy garnet may be marked by either very sharp or smooth compositional changes (Figure 6).

Porphyroblasts that are dominated by cloudy garnet may have a relatively clear Ca-rich inner rim (Figures 6 and 7) that is matched by slightly lower concentrations of the other divalent cations. The inner rim zones have the highest Ca contents when they are most distant from any clear garnet rims at either the porphyroblast edge or any sillimanite-bearing inclusions (Figures 6b and 8). These Ca-rich zones are truncated by sillimanite-bearing embayments at the edge of porphyroblasts in ugr0 (Figure 7a). In these parts of porphyroblasts, textures are intermediate between cloudy and clear end-members, with small mineral inclusions but moderate concentrations of small fluid inclusions. Unlike the adjacent areas of cloudy garnet, these inclusions do not form with an obvious crystallographic alignment. Such Ca-rich zones are absent from porphyroblasts that contain very dark cloudy garnet textures in the rim parts of porphyroblasts (Figure 7b).

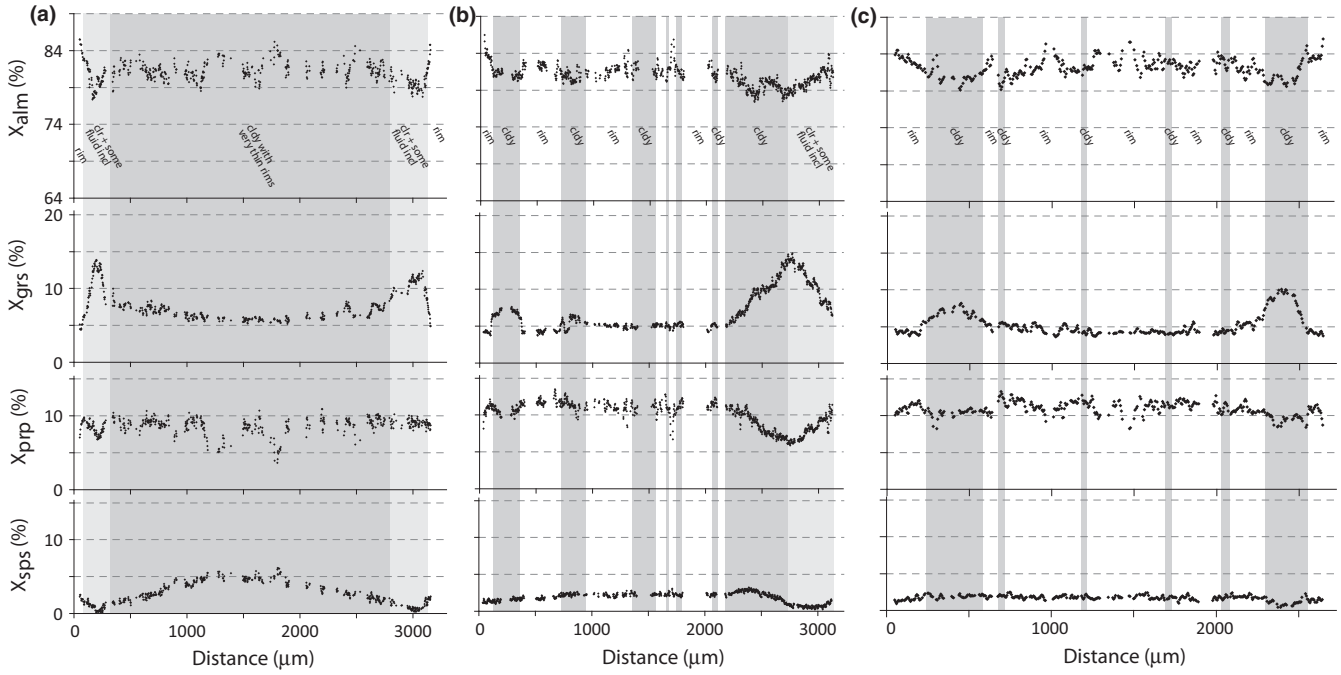

FIGURE 6 Compositional zoning profiles of dominantly cloudy garnet. (a) ugr1 Grt 3 with very thin clear rims adjacent to some inclusions and matrix. (b) ugr0 c4 with wide clear rims adjacent to most inclusions (Sil-bearing). (c) ugr0 c1 with wide clear rims adjacent to most inclusions and matrix (Sil-bearing)

4.3 | Clear rims

The clear rims tend to have a relatively consistent composition with ~4.5 mol.% grosssular, 10 mol.% pyrope and 84 mol.% almandine (Figure 8). Mn contents are typically low but a little more variable at porphyroblast edges, which may show a local enrichment (De Béthune, Laduron, & Bocquet, 1975). There are no local compositional differences at the edge of the garnet porphyroblasts that appear to correlate with the nature of the matrix phase (Figure 9). Transitions between clear rims and cloudy garnet are typically very sharp with a sudden change at the margin,

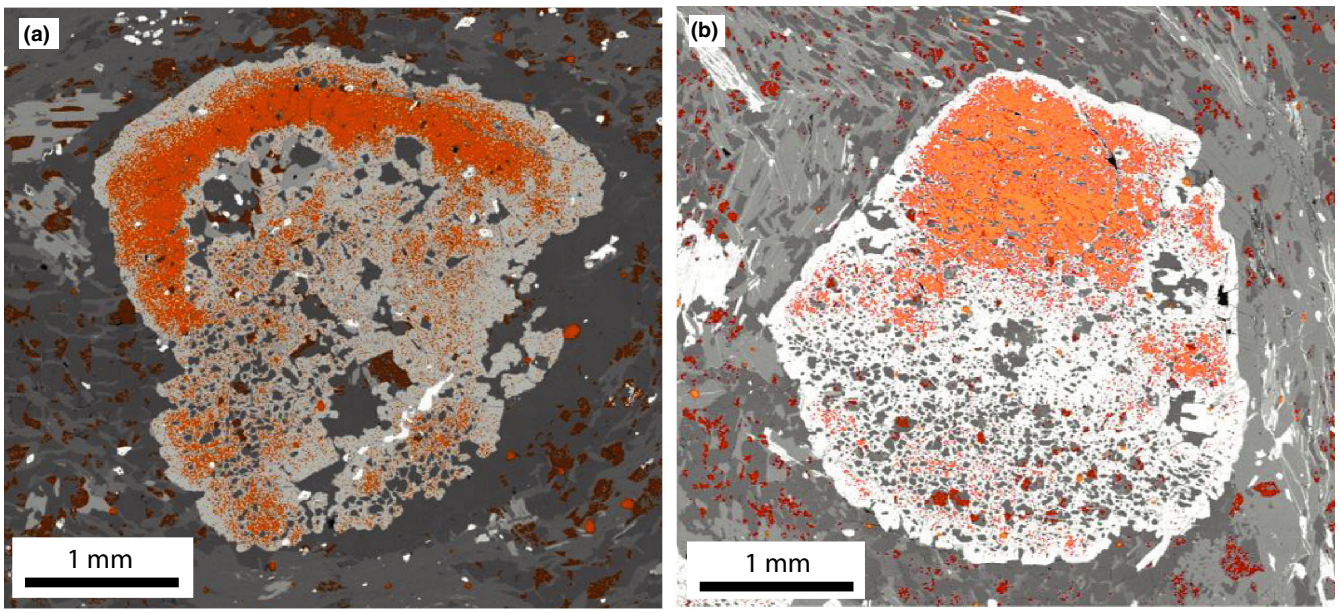

FIGURE 7 (a) Mixed backscattered electron (BSE) image and X-ray map of Ca for garnet porphyroblast (ugr0 c2) showing irregular right-hand edge of dominantly cloudy garnet porphyroblast associated with sillimanite-rich embayments and truncation of Ca-rich (orange colours) inner rim. (b) Mixed BSE image and X-ray map of Ca for garnet porphyroblast (ugr1 Grt7) with inclusion-rich cloudy garnet in lower part of the image adjacent to Ca-rich clear garnet (upper part) with thin Ca-poor rim [Colour figure can be viewed at wileyonlinelibrary.com]

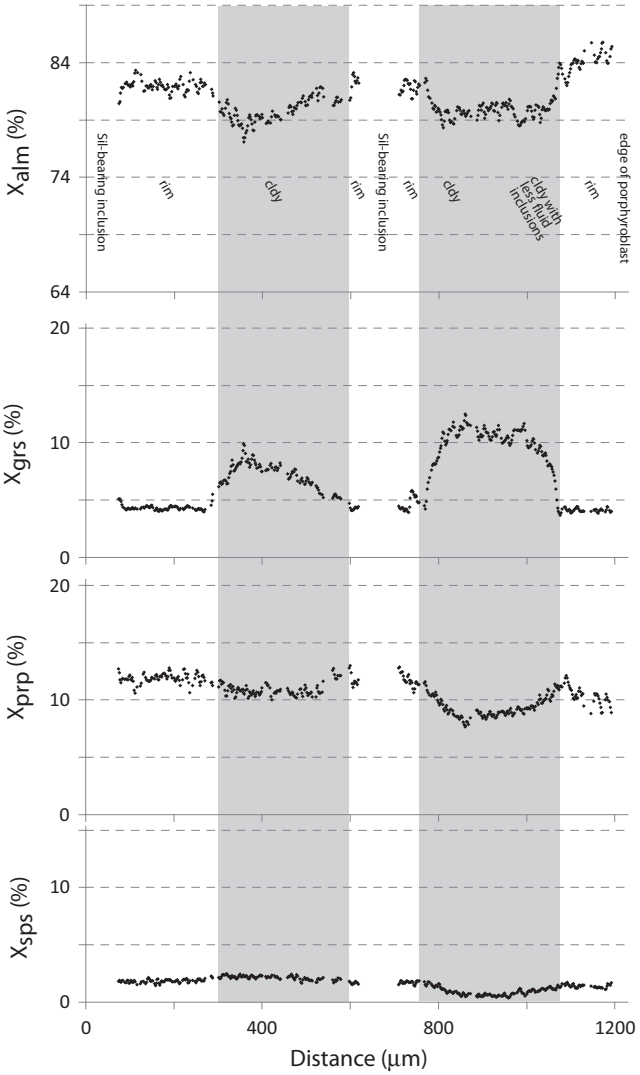

FIGURE 8 Compositional zoning profile of clear rims adjacent to both matrix and sillimanite-bearing inclusions within dominantly cloudy (cldy) garnet (ugr0 c4)

although some smoothing of this transition occurs within the cloudy garnet relative to the more uniform compositions of the clear rim garnet (Figure 8).

5 | INTERPRETATION

5.1 | Garnet characteristics

Large garnet porphyroblasts with typical Mn- and Ca-rich cores and a gradual increase in Mg/Fe towards the rim are dominated by clear garnet with small, typically quartz inclusions. These are interpreted as preserving the earliest stage of garnet growth during prograde metamorphism and are typical of porphyroblasts from regional metamorphic garnet zone assemblages (e.g. Hollister, 1966; Phillips et al., 1994). Clear garnet is typically best preserved in ugr1 where less modification has occurred associated with the growth of

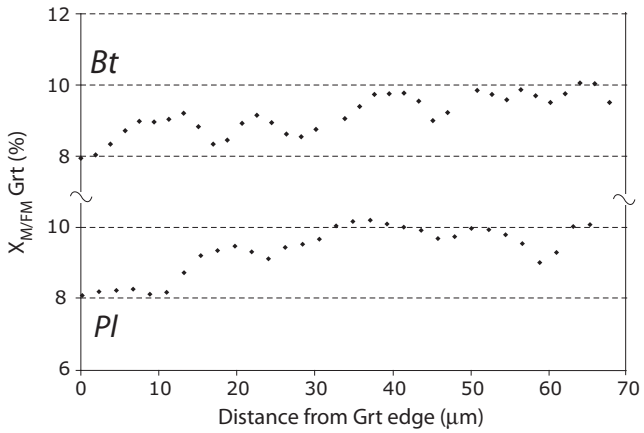

FIGURE 9 Comparison of the compositional zoning profiles at the edge of garnet porphyroblast adjacent to biotite (Bt) and plagioclase (Pl)

sillimanite. Many of the porphyroblasts in both samples have either been partially or completely modified by the processes forming cloudy garnet (Hames & Menard, 1993; Martin et al., 2011; Whitney, Mechum, Dilek, & Kuehner, 1996), as is reported in the Leven Schists towards the southwest (Dempster, La Piazza, et al., 2017). The cloudy garnet with crystallographically aligned fluid inclusions is thought to represent a patchy to complete alteration via a dissolution–reprecipitation mechanism (Dempster, La Piazza, et al., 2017; Erambert & Austrheim, 1993; Putnis & Putnis, 2007; Ruiz-Agudo, Putnis, & Putnis, 2014) associated with the generation of large irregular quartz inclusions. This process causes partial re-equilibration of garnet producing variable compositions both within and between individual porphyroblasts, and between adjacent rocks (Dempster, La Piazza, et al., 2017). Where patchy alteration occurs, the cloudy garnet inherits a partially modified chemistry from the local composition of the original porphyroblast. In instances where replacement of the whole porphyroblast occurs typically rather uniform compositions are produced, perhaps with a vestige of the original bell-shaped Mn profile (Figure 5).

Formation of cloudy garnet involves some consumption of garnet, associated with the increase in modal proportion of inclusions from ~5% in the original clear garnet to ~25% inclusions in the cloudy garnet. This represents an absolute reduction of about ~0.8 vol.% (i.e. original 5.2% to the present 4.4%) garnet in ugr1 and 1.4 vol.% (i.e. original 10% to the present 8.6% garnet) loss of garnet from ugr0. In Leven schists to the southwest, cloudy garnet is linked to the production of staurolite (Dempster, La Piazza, et al., 2017). This is associated with the following reaction:

$$\mathrm{Grt_{(clear)}} + \mathrm{Ms} + \mathrm{H_2O} = \mathrm{Grt_{(cloudy)}} + \mathrm{St} + \mathrm{Bt} + \mathrm{Qz}.$$

The evidence for this reaction is preserved in our samples from the spatial association between the garnet

porphyroblasts and staurolite (Figure 2a). There is also a general correlation between garnet consumption and staurolite production; however, the very small amounts of staurolite in ugr1 and the important role of fluids in the generation of cloudy garnet suggest that there may be an element of open system behaviour in the generation of staurolite (Dempster, La Piazza, et al., 2017) that is most evident with relatively small amounts of reaction. The composition of garnet lost in this reaction is hard to estimate and so balancing the reaction is difficult.

The formation of cloudy garnet is an effective mechanism of generating relatively flat compositional profiles that is potentially independent of any volume diffusion driven process (cf. Ague & Axler, 2016; Ague & Baxter, 2007; Dempster, 1985; Viete et al., 2011). Although flat compositional profiles and variable profiles within single rocks may be manifestations of thin section cuts and or variable timing of porphyroblast growth, this cannot explain the characteristics of individual porphyroblasts (e.g. Figure 7b). Hence, resetting of garnet composition by coupled dissolution–reprecipitation introduces an additional element of caution in the interpretation that flat zoning profiles are a result of effective volume diffusion and the application of thermodynamic-based models to estimate initial zoning profiles in garnet (Spear et al., 1990). Decoupling of Ca distribution from that of Mn and Mg has been interpreted as a reflection of sluggish volume diffusion of Ca within garnet relative to the other cations (Tuccillo, Essene, & van der Pluijm, 1990). Indeed such inferences have been used by Viete et al. (2011) as robust lines of evidence for Mn diffusion in garnet. During partial resetting due to a coupled dissolution–reprecipitation mechanism, Ca appears to show the most marked re-equilibration (Figure 5). This could be indicative of a partial re-equilibration in response to falling pressure associated with the reaction (Holdaway, 2001) rather than any major change in temperature.

Ca-rich marginal areas of dominantly cloudy garnet porphyroblasts (Figures 6 and 7) typically have lower concentrations of fluid inclusions and these rarely show evidence of alignment. They pre-date the replacement by sillimanite (Figure 7b) and are thought to represent parts of the porphyroblast that have only experienced limited compositional change during the coupled dissolution–reprecipitation process. However, they are in sufficiently close proximity to cloudy garnet to have been influenced by the introduction of fluid. Gradual changes in composition are observed at the margins of these Ca-rich zones (Figure 8) and could be indicative of relatively slow diffusion of Ca, in an attempt to equilibrate to clear rim composition during the formation of sillimanite. Hence, Ca appears to preserve this vestige of the original zoning in these areas, in contrast to the other divalent cations, and is perhaps indicative of such areas being more resistant to cloudy garnet formation. Some diffusional modification of these profiles also may have occurred. Such Ca-rich zones appear to be ubiquitous based on the evidence presented in Figure 6, however, this is not the case (Figure 7b). There is an element of sampling bias represented in the zoning profiles (Figure 6), as transects were often chosen to pass through garnet-dominated parts of each porphyroblast rather than inclusion-rich edge areas.

Detailed zoning profiles at the edges of the garnet porphyroblasts show no systematic difference in the compositions of the garnet that are linked to the nature of the adjacent matrix phase (Figure 9) and as such there is no evidence of low-T retrograde diffusive exchange between the garnet and biotite (Mueller et al., 2010; Tracy, Robinson, & Thompson, 1976). The presence of irregular and sharp compositional gradients between cloudy garnet and clear garnet throughout the zoning profiles (Figures 5, 6 and 8) also indicates that volume diffusion is not a major influence on the compositional profiles of the garnet.

The production of cloudy garnet via a coupled dissolution–reprecipitation mechanism produces an element a partial re-equilibration in the garnet compositions that will then influence all subsequent garnet-consuming reactions.

5.2 | Sillimanite-producing reaction

The production of sillimanite in these rocks is strongly linked to the partial dissolution of the garnet, most typically around the central parts of porphyroblasts where atoll-like shapes may be produced around inclusions of sillimanite, quartz and coarse biotite (Figure 3j). Similar textures are commonly reported in other studies (e.g. Yardley, 1977b). The reaction is also associated with the formation of clear inclusion-free rims that have also been reported in other locations (Dempster, La Piazza, et al., 2017; Martin et al., 2011; Mueller et al., 2010; Whitney et al., 1996) around both the edges of the porphyroblast and the edges of sillimanite-bearing inclusions (Figure 3f). There is a strong correlation between the amount of sillimanite that forms and the width of these clear zones (Figure 4b). This relationship varies between individual porphyroblasts and so the production of sillimanite appears to be strongly controlled by the nature of the individual garnet porphyroblast. There also appears to be a deformation control on the reaction as the most prominent clusters of sillimanite are strongly linked to specific positions around each individual garnet porphyroblast nearest to the cleavage domain (Figures 1b and 2b). These clusters form not just where muscovite is in contact with the edge of the porphyroblast but tend to be at an angle of 30° to the orientation of σ_1 for the cleavage (Figure 2b), implying a link to active shear. Clear rims are more prominently developed adjacent to sillimanite-bearing matrix rather than sillimanite-bearing

inclusions (Figure 4b), indicating an important role for matrix phases in the isograd reaction. There is an order of magnitude less sillimanite produced in the sample that contains the highest proportion of clear 'unmodified' original garnet (Table 1). As such the porous, cloudy garnet is most obviously modified (cf. Jonas, Müller, Dohmen, Immenhauser, & Putlitz, 2017) by the sillimanite-producing event. Garnet appears to be both consumed in this reaction and new garnet is precipitated producing the clear rims at the reaction front (cf. Jonas et al., 2017; Putnis, 2009). Although the nature of the inclusions within the garnet is modified, the overall volume of inclusions only shows a slight (~1 vol.%) absolute change from ugr1 to ugr0. Thus, only a small amount of garnet is consumed in the sillimanite isograd reaction, consistent with the relatively small modal percentage of sillimanite that is produced (Table 1).

Based on the textures preserved, the production of sillimanite and biotite from garnet is inferred to be associated with the following reaction:

$$\mathrm{Grt_{(cloudy)}} + \mathrm{Ms} = \mathrm{Grt_{(clear)}} + \mathrm{Sil} + \mathrm{Bi} + \mathrm{Qz}$$

This is a continuous reaction in KFMASH systems (Holdaway, Guidotti, Novak, & Henry, 1982). Muscovite is very rarely present as inclusions in the garnet and so its involvement must be solely as a matrix phase. This accounts for the relatively wide rims of clear garnet adjacent to the matrix in comparison to inclusions (Figure 4b). Significant mobility of some components must take place to allow the reaction to occur with apparently isolated inclusions (Carmichael, 1969; Foster, 1977; Yardley, 1977b). In theory, sillimanite-producing reactions that consume garnet only occur once staurolite breakdown has occurred (Holdaway et al., 1982; Pattison & Tinkham, 2009). However, there is no obvious effect on the morphology of staurolite (Figure 3i), which, based on theoretical petrogenetic grid constraints (Harte & Hudson, 1979; Spear & Cheney, 1989; Thompson, 1976), might be interpreted as metastable perhaps due to its zinc content (Ashworth, 1975). However, Zn contents are less than 0.5% and so it seems possible that there are kinetic impediments to staurolite reaction. Despite the relatively high pressures of regional metamorphism that have been determined for the area (Phillips et al., 1994), no kyanite has been reported. However, *P–T* determination and indeed meaningful isograd maps depend on equilibrium being attained and this has not typically occurred.

The variable development of sillimanite both within and between individual samples might be interpreted as a reflection of compositional control as the rocks have experienced identical pressure and temperature conditions. The process of partial equilibration during the formation of cloudy garnet results in a wide range of disequilibrium garnet compositions within an individual porphyroblast and sample. In theory, the sillimanite-producing reaction is dependent on garnet Mn- and Ca contents (Mahar, Baker, Powell, Holland, & Howell, 1997). Others have interpreted atoll-like garnet textures to reflect the preferential consumption of low temperature Mn-rich growth zones from the central parts of porphyroblasts (Cheng, Nakamura, Kobayashi, & Zhou, 2007). However, sillimanite production is most strongly associated with cloudy garnet that has largely lost its original low temperature core compositions. Sillimanite also occurs in inclusions in ugr0 close to cloudy garnet with a range of Ca contents and is not linked to especially low Mn areas. Hence, there appear to be no systematic compositional differences within or between the two samples that could explain the local differences in amount of sillimanite that formed. Sillimanite introduction appears to be linked to a partial dissolution of cloudy garnet, a purge in the fluid inclusion content (Putnis, Tsukamoto, & Nishimura, 2005) of the immediately adjacent cloudy garnet and the reprecipitation of garnet rims with a relatively Ca-poor composition. As such, fluids seem to be of more significance to this reaction than any subtleties associated with local garnet composition.

The reaction generally occurs around the porphyroblast margins, within embayments, but also in larger, possibly interconnected inclusions. Some sillimanite is also present in apparently isolated quartz inclusions in areas of otherwise clear garnet. Although this may be a 2D artefact of the sectioning, in most such instances, these inclusions occur close to prominent fractures within the porphyroblast and this suggests that some of these fractures are early features of the texture and may reflect areas where fluids have catalysed the reaction and delivered and removed more mobile components (Whitney, 1996; Whitney, Cooke, & Du Frane, 2000). The deflection of cloudy garnet-clear rim textural transitions associated with some fractures (Figure 2h) also suggests that these are peak metamorphic features of the garnet porphyroblasts.

5.3 | Reaction controls and internal metasomatism

The localized formation of cloudy garnet (Dempster, La Piazza, et al., 2017) results in a combination of patches of cloudy textures with variable compositions and original clear garnet partly retaining concentric growth zoning patterns. The inability to equilibrate seems to be a key in understanding the subsequent metamorphic development. Cloudy garnet appears to be inherently more reactive than the clear garnet, despite the cores of the former being potentially most out of equilibrium at the higher temperatures. The production of staurolite has locally generated garnet textures (Dempster, La Piazza, et al., 2017) that are more prone to the sillimanite reaction (i.e. more cloudy

garnet), but also more biotite, that may then create a different response to deformation. The textural and rheological variability created during this event appears to have controlled the subsequent reaction to produce sillimanite, which further enhances the textural and geochemical variability. The preferential formation of sillimanite at the margins of the garnet in specific positions relative to the cleavage in the schists also points towards deformation providing a crucial trigger for the sillimanite isograd reaction.

Kyanite is not produced in this reaction history and most notably staurolite breakdown does not occur. This suggests that these reactions may be kinetically challenging (Mueller et al., 2010), despite the likely high reaction affinity (cf. Pattison, De Capitani, & Gaidies, 2011). Hence, an equilibrium thermodynamic-based model of prograde evolution (e.g. Spear & Cheney, 1989; Wei, Powell, & Clarke, 2004) may be problematic in these rocks. Conditions during peak metamorphic temperatures may be dominated by falling pressure (England & Thompson, 1984) and as such some key temperature sensitive reactions may not be significantly overstepped, in contrast to the pressure-sensitive reactions discussed in this study (Figure 10).

Internal metasomatism (cf. Spear, 1988) will occur associated with the production of cloudy garnet via coupled dissolution–reprecipitation. The effect of this will be to make the effective equilibrium whole-rock composition more Ca-, Mn-rich and Mg-poor. With a prograde heating path, this change in composition will in theory inhibit the formation of sillimanite by the observed reaction (Holdaway et al., 1982). This does not seem to have occurred as a lower proportion of sillimanite is produced in the rocks that contain the least modified garnet. However, the influence of internal metasomatism may be crucial in controlling reaction pathways as staurolite introduction may initially occur under relatively Ca- and Mn-poor conditions (i.e. high *P*) associated with largely closed system garnet. On formation of cloudy garnet the whole rock becomes effectively Ca- and Mn-rich and garnet breakdown to form sillimanite will occur at lower pressures (Figure 10). Consequently, a 'conventional' *P–T–t* loop (England & Thompson, 1984) is capable of passing through both the staurolite- and sillimanite-producing reactions (Figure 10), which would be impossible without a significant change in the effective whole-rock composition. Such shifts in the reaction position in *P–T* space may be significant in controlling the relative amounts of sillimanite reaction that have occurred in these rocks.

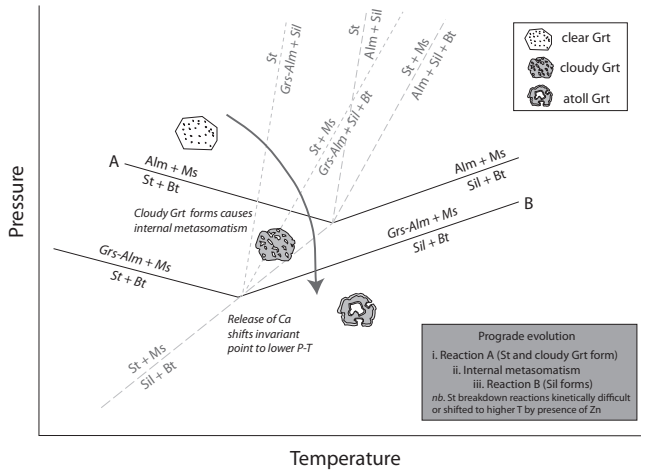

FIGURE 10 Partial KFMASH petrogenetic grid (after Holdaway et al., 1982) highlighting the influence of the development of cloudy garnet, internal Ca-metasomatism and inferred kinetically difficult reactions on the prograde evolution of the Leven schists. Cartoons show the changes in garnet textures associated with each reaction. Reaction lines in black are responsible for the introduction of staurolite and sillimanite with consumption of both an Fe-rich garnet (Alm) and a more Ca-rich garnet (Grs–Alm). Reaction lines in grey no evidence observed in the rocks. Arrow shows inferred *P–T*–time path

A number of interrelated steps appear to control the sillimanite isograd reaction in these rocks. Only individual garnet porphyroblasts that contain abundant cloudy garnet, with relatively Ca-rich original core compositions, will experience large shifts in composition that may move the invariant point to low enough pressure and temperature (Figure 10). In addition, both sillimanite- and staurolite-producing reactions appear to be triggered by deformation. Hence, the kinetic controls on the formation of cloudy garnet are crucial in controlling the subsequent formation of sillimanite. The influence of Mn on the reaction topology will be relatively small by comparison because, in contrast to Ca, Mn appears to be preferentially partitioned back into the garnet during the coupled dissolution–reprecipitation process (Dempster, La Piazza, et al., 2017).

The influence of chemical fractionation on pressure–temperature pseudosections during garnet growth has been considered (Spear & Wolfe, 2018; Tinkham & Ghent, 2005; Vance & Mahar, 1998; Zuluaga, Stowell, & Tinkham, 2005). However, changes in the effective whole-rock composition due coupled dissolution–reprecipitation are more likely to influence the metamorphic evolution and create problems with equilibrium thermodynamic approaches (Wei et al., 2004). Reaction-driven internal metasomatism may be short-lived in comparison to changes in the effective bulk rock composition caused by either fractionation during porphyroblast growth (Zuluaga et al., 2005) or subsequent diffusive re-equilibration of porphyroblasts (Spear, 1988). Given the variety of chemically zoned minerals present in pelites, in addition to garnet (e.g. plagioclase, muscovite, staurolite), such behaviour may be a common control on reaction grid topology that should be considered.

5.4 | A general model of prograde evolution of garnet porphyroblasts

The following prograde evolution of garnet is suggested here. It is important to emphasize that there is nothing obviously unusual about these lithologies and so this type of general evolution may well be typical of amphibolite facies garnet porphyroblasts in regionally metamorphosed mica schist. Possible mechanisms by which garnet may participate in metamorphic reactions include: diffusion (Carlson, 2006), dissolution (Kohn & Malloy, 2004) or coupled dissolution–reprecipitation (Erambert & Austrheim, 1993).

Garnet grows at lower grades with typical bell-shaped prograde Mn profiles (e.g. Hollister, 1966), controlled by enhanced partitioning of Mn into garnet at lower temperatures (Dempster, La Piazza, et al., 2017). Essentially, this may be an equilibrium growth process; however, because of sluggish volume diffusion much of the subsequent re-equilibration or reaction of garnet is only possible with kinetic enhancement. With the local introduction of fluids at elevated temperature, garnet may partially or completely equilibrate by a coupled dissolution–reprecipitation mechanism to produce patches of cloudy garnet and in some cases flat zoning profiles characterized by a higher temperature geochemistry. This mechanism might also be considered as a potential explanation of patchy Ca and Mn domains in garnet porphyroblasts (cf. Carlson, 2002; Chernoff & Carlson, 1997; Hirsch, Prior, & Carlson, 2003). Coupled dissolution–reprecipitation may occur associated with particular isograd reactions to produce staurolite (Dempster, La Piazza, et al., 2017), but assemblage change reactions may not be a requirement. This localized early modification of garnet appears to be enhanced by deformation-enhanced fluid access to parts of the porphyroblasts. With further prograde metamorphism, this cloudy garnet is more prone to subsequent reactions that are triggered by deformation (Dempster & Tanner, 1997) and enhanced by the presence of the fluid inclusions within the porous reactant garnet (Jonas et al., 2017; Putnis & Austrheim, 2010; Rubie, 1986). The cloudy garnet is also characterized by larger mineral inclusions, which may provide a focus for later deformation and fluid influx (Whitney et al., 2000). The extent of metasomatic change associated with the formation of cloudy garnet plays a crucial role in the subsequent reaction history.

Coupled dissolution–reprecipitation represents a prograde reaction mechanism that occurs unevenly within garnet porphyroblasts due to its localized controls. Different elements are subject to different levels of equilibration and hence preserve different scales of disequilibrium (Carlson, 2002), although in this instance different rates of intergranular diffusion are not the crucial factor. The resulting compositional and textural characteristics then have a major influence on subsequent reaction history and 'peak metamorphic' character.

6 | CONCLUSIONS

- The chemical and textural variability of garnet highlights the danger of interpreting *P–T* histories based on the zoning profiles of individual porphyroblasts.
- 'Flat' garnet zoning profiles may form by coupled dissolution–reprecipitation processes and need not be generated by effective volume diffusion.
- Internal metasomatism will occur associated with coupled dissolution–reprecipitation of chemically zoned garnet. Such compositional changes may significantly change reaction pathways.
- Kinetic factors are dominant controls on reaction progress in both the production of staurolite (Dempster, La Piazza, et al., 2017) and the development of sillimanite. Many prograde reactions may be limited by kinetic restrictions of the reactants. Whilst petrogenetic reaction grids (e.g. Spear & Cheney, 1989) provide a valuable framework of theoretical relationships, a rethink may be required based on the kinetic responses of the reactants.
- Local variations in the characteristics of individual garnet porphyroblasts control their reaction history. This results in a lack of equilibrium between adjacent porphyroblasts and a lack of equilibrium between adjacent metamorphic rocks. Consequently, the concept of progressive equilibration during metamorphism is questioned in these amphibolite facies rocks. Hence, on both regional and local scales, assemblages may be inconsistent with the peak metamorphic conditions. There is a common assumption that equilibrium will be readily achieved during regional metamorphism due to the long time-scales, presence of fluids and active deformation (e.g. Martin et al., 2011; Pattison & Tinkham, 2009). This assumption may be flawed.

ACKNOWLEDGEMENTS

J. Gilleece is thanked for technical assistance. J. Faithfull is thanked for initially drawing our attention to the presence of sillimanite in the upper reaches of Glen Roy. T. Müller is thanked for his very constructive review and an anonymous reviewer for their insightful comments.

CONFLICT OF INTEREST

The authors have no conflicts of interest.

ORCID

Tim J. Dempster http://orcid.org/0000-0002-2334-7977

REFERENCES

Ague, J. J., & Axler, J. A. (2016). Interface coupled dissolution-reprecipitation in garnet from subducted granulites and ultrahigh-pressure rocks revealed by phosphorous, sodium, and ititanium zonation. *American Mineralogist*, *101*, 1696–1699. https://doi.org/10.2138/am-2016-5707

Ague, J. J., & Baxter, E. F. (2007). Brief thermal pulses during mountain building recorded by Sr diffusion in apatite and multicomponent diffusion in garnet. *Earth and Planetary Science Letters*, *261*, 500–516. https://doi.org/10.1016/j.epsl.2007.07.017

Ashworth, J. R. (1975). Staurolite at anomalously high grade. *Contributions to Mineralogy and Petrology*, *53*, 281–291. https://doi.org/10.1007/BF00382444

Atherton, M. P. (1968). The variation in garnet, biotite and chlorite composition in medium grade pelitic rocks form the Dalradian, Scotland, with particular reference to the zonation in garnet. *Contributions to Mineralogy and Petrology*, *18*, 347–371. https://doi.org/10.1007/BF00399696

Barrow, G. (1893). On an intrusion of muscovite-biotite gneiss in the southeastern Highlands of Scotland and its accompanying metamorphism. *Quarterly Journal of the Geological Society, London*, *49*, 330–358. https://doi.org/10.1144/GSL.JGS.1893.049.01-04.52

Bell, T. H., & Johnson, S. E. (1989). Porphyroblast inclusion trails: The key to orogensis. *Journal of Metamorphic Geology*, *7*, 279–310. https://doi.org/10.1111/j.1525-1314.1989.tb00598.x

Borinski, S. A., Hoppe, U., Chakraborty, S., Ganguly, J., & Bhowmik, S. K. (2012). Multicomponent diffusion in garnets I: General theoretical consideration and experimental data for Fe-Mg systems. *Contributions to Mineralogy and Petrology*, *164*, 571–586. https://doi.org/10.1007/s00410-012-0758-0

Caddick, M. J., Konopásek, J., & Thompson, A. B. (2010). Preservation of garnet growth zoning and the duration of prograde metamorphism. *Journal of Petrology*, *51*, 2327–2347. https://doi.org/10.1093/petrology/egq059

Carlson, W. D. (2002). Scales of disequilibrium and rates of equilibration during metamorphism. *American Mineralogist*, *87*, 185–204. https://doi.org/10.2138/am-2002-2-301

Carlson, W. D. (2006). Rates of Fe, Mg, Mn, and Ca diffusion in garnet. *American Mineralogist*, *91*, 1–11. https://doi.org/10.2138/am.2006.2043

Carlson, W. D., Hixon, J. D., Garber, J. M., & Bodnar, R. J. (2015). Controls on metamorphic equilibration: The importance of intergranular solubilities mediated by fluid composition. *Journal of Metamorphic Geology*, *33*, 123–146. https://doi.org/10.1111/jmg.12113

Carlson, W. D., Pattison, D. R. M., & Caddick, M. J. (2015). Beyond the equilibrium paradigm: How consideration of kinetics enhances metamorphic interpretation. *American Mineralogist*, *100*, 1659–1667. https://doi.org/10.2138/am-2015-5097

Carmichael, D. M. (1969). On the mechanism of prograde metamorphic reactions in quartz-bearing pelitic rocks. *Contributions to Mineralogy and Petrology*, *20*, 244–267. https://doi.org/10.1007/BF00377479

Cheng, H., Nakamura, E., Kobayashi, K., & Zhou, Z. (2007). Origin of atoll garnets in eclogites and implications for the redistribution of trace elements during slab exhumation in a continental subduction zone. *American Mineralogist*, *92*, 1119–1129. https://doi.org/10.2138/am.2007.2343

Chernoff, C. B., & Carlson, W. D. (1997). Disequilibrium for Ca during growth of pelitic garnet. *Journal of Metamorphic Geology*, *15*, 421–438. https://doi.org/10.1111/j.1525-1314.1997.00026.x

Chu, X., & Ague, J. J. (2015). Analysis of experimental data on divalent cation diffusion kinetics in aluminosilicate garnets with application to timescales of peak Barrovian metamorphism, Scotland. *Contributions to Mineralogy and Petrology*, *170*, 25. https://doi.org/10.1007/s00410-015-1175-y

De Béthune, P., Laduron, D., & Bocquet, J. (1975). Diffusion processes in resorbed garnets. *Contributions to Mineralogy and Petrology*, *50*, 197–204. https://doi.org/10.1007/BF00371039

Dempster, T. J. (1985). Garnet zoning and metamorphism of the Barrovian Type Area, Scotland. *Contributions to Mineralogy and Petrology*, *89*, 30–38. https://doi.org/10.1007/BF01177588

Dempster, T. J., & Harte, B. (1986). Polymetamorphism in the Dalradian of the central Scottish Highlands. *Geological Magazine*, *123*, 95–104. https://doi.org/10.1017/S0016756800029757

Dempster, T., & Jess, S. A. (2015). Ikaite pseudomorphs in Neoproterozoic Dalradian slates record Earth's coldest metamorphism. *Journal of the Geological Society, London*, *172*, 459–464. https://doi.org/10.1144/jgs2015-018

Dempster, T. J., La Piazza, J., Taylor, A., Beaudoin, N., & Chung, P. (2017). Chemical and textural equilibration of garnet during amphibolite facies metamorphism: The influence of coupled dissolution–reprecipitation. *Journal of Metamorphic Geology*, *36*, 1–20.

Dempster, T. J., Rogers, G., Tanner, P. W. G., Bluck, B. J., Muir, R. J., Redwood, S. D., … Paterson, B. A. (2002). Timing of deposition, orogenesis and glaciation within the Dalradian rocks of Scotland: Constraints from U-Pb ages. *Journal of the Geological Society, London*, *159*, 83–94. https://doi.org/10.1144/0016-764901061

Dempster, T. J., Symon, S., & Chung, P. (2017). Intergranular diffusion rates from the analysis of garnet surfaces: Implications for metamorphic equilibration. *Journal of Metamorphic Geology*, *35*, 585–600. https://doi.org/10.1111/jmg.12247

Dempster, T. J., & Tanner, P. W. G. (1997). The biotite isograd, Central Pyrenees: A deformation-controlled reaction. *Journal of Metamorphic Geology*, *15*, 531–548. https://doi.org/10.1111/j.1525-1314.1997.00039.x

England, P. C., & Thompson, A. B. (1984). Pressure-temperature-time paths of regional metamorphism I. Heat transfer during the evolution of regions of thickened continental crust. *Journal of Petrology*, *25*, 894–928. https://doi.org/10.1093/petrology/25.4.894

Erambert, M., & Austrheim, H. (1993). The effect of fluid and deformation on zoning and inclusion patterns in poly-metamorphic garnets. *Contributions to Mineralogy and Petrology*, *115*, 204–214. https://doi.org/10.1007/BF00321220

Foster, C. T. (1977). Mass transfer in sillimanite-bearing pelitic schists near Rangeley, Main. *American Mineralogist*, *62*, 727–746.

Ganguly, J. (2010). Cation diffusion kinetics in aluminosilicate garnets and geological applications. *Reviews in Mineralogy and Geochemistry*, *72*, 559–601. https://doi.org/10.2138/rmg.2010.72.12

Hames, W. E., & Menard, T. (1993). Fluid-assisted modification of garnet composition along rims, cracks, and mineral inclusion boundaries in samples of amphibolite facies schists. *American Mineralogist*, *78*, 338–344.

Harris, A. L., Haselock, P. J., Kennedy, M. J., & Mendum, J. R. (1994). The Dalradian Supergroup in Scotland, Shetland and Ireland. In A. L. Harris & W. Gibbons (Eds.), *A revised correlation of Precambrian rocks in the British Isles*. *Geological Society, London*, Special Report, *22*, 33–53. https://doi.org/10.1144/SR22

Harte, B., & Henley, K. J. (1966). Occurrence of compositional zoned almanditic garnets in regionally metamorphosed rocks. *Nature*, *210*, 689–692. https://doi.org/10.1038/210689a0

Harte, B., & Hudson, N. F. C. (1979). Pelite facies series and the temperatures and pressures of Dalradian metamorphism in E. Scotland. In A. L. Harris, C. H. Holland & B. E. Leake (Eds.) *The Caledonides of the British Isles — Reviewed*. *Geological Society of London Special Publication*, *8*, 323–337.

Hirsch, D. M., Prior, D. J., & Carlson, W. D. (2003). An overgrowth model to explain multiple, dispersed high-Mn regions in the cores of garnet porphyroblasts. *American Mineralogist*, *88*, 131–141. https://doi.org/10.2138/am-2003-0116

Holdaway, M. J. (2001). Recalibration of the GASP geobarometer in the light of recent garnet and plagioclase activity models and versions of the garnet-biotite geothermometer. *American Mineralogist*, *86*, 1117–1129. https://doi.org/10.2138/am-2001-1001

Holdaway, M. J., Guidotti, C. V., Novak, J. M., & Henry, W. E. (1982). Polymetamorphism in medium- to high-grade pelitic metamorphic rocks, west-central Maine. *Geological Society of America, Bulletin*, *93*, 572–584. https://doi.org/10.1130/0016-7606(1982)93<572:PIMTHP>2.0.CO;2

Hollister, L. S. (1966). Garnet zoning: An interpretation based on the Rayleigh fractionation model. *Science*, *154*, 1647–1651. https://doi.org/10.1126/science.154.3757.1647

Jonas, L., Müller, T., Dohmen, R., Immenhauser, A., & Putlitz, B. (2017). Hydrothermal replacement of biogenic and abiogenic aragonite by Mg-carbonate – Relation between textural control on effective element fluxes and resulting carbonate phase. *Geochimica et Cosmochimica Acta*, *196*, 289–306. https://doi.org/10.1016/j.gca.2016.09.034

Kohn, M. J. (2014). Geochemical zoning in metamorphic minerals. *Treatise on Geochemistry*, *4*, 249–280. https://doi.org/10.1016/B978-0-08-095975-7.00307-7

Kohn, M. J., & Malloy, M. A. (2004). Formation of monazite via prograde metamorphic reactions among common silicates: Implications for age determinations. *Geochimica et Cosmochimica Acta*, *68*, 101–113. https://doi.org/10.1016/S0016-7037(03)00258-8

Lasaga, A. C. (1983). Geospeedometry: An extension of geothermometry. In: S. K. Saxena (Ed.), *Kinetics and equilibrium in mineral reactions. Advances in Physical Geochemistry, v. 3* (pp. 81–114). New York, NY: Springer. https://doi.org/10.1007/978-1-4612-5587-1

Mahar, E. M., Baker, J. M., Powell, R., Holland, T. J. B., & Howell, N. (1997). The effect of Mn on mineral stability in metapelites. *Journal of Metamorphic Geology*, *15*, 223–238. https://doi.org/10.1111/j.1525-1314.1997.00011.x

Martin, L. A. J., Ballèvre, M., Boulvais, P., Halfpenny, A., Vanderhaeghe, O., Duchêne, S., & Deloule, E. (2011). Garnet re-equilibration by coupled dissolution-reprecipitation: Evidence from textural, major element and oxygen isotope zoning of 'cloudy' garnet. *Journal of Metamorphic Geology*, *29*, 213–231. https://doi.org/10.1111/j.1525-1314.2010.00912.x

Moynihan, D. P., & Pattison, D. R. M. (2013). An automated method for the calculation of P-T paths from garnet zoning, with application to metapelitic schist from the Kootenay Arc, British Columbia, Canada. *Journal of Metamorphic Geology*, *31*, 525–548. https://doi.org/10.1111/jmg.12032

Mueller, T., Watson, E. B., & Harrison, T. M. (2010). Application of diffusion data to high temperature earth systems. *Reviews in Mineralogy and Geochemistry*, *72*, 997–1038. https://doi.org/10.2138/rmg.2010.72.23

Pattison, D. R. M., De Capitani, C., & Gaidies, F. (2011). Petrological consequences of variations in metamorphic reaction affinity. *Journal of Metamorphic Geology*, *29*, 953–977. https://doi.org/10.1111/j.1525-1314.2011.00950.x

Pattison, D. R. M., & Tinkham, D. K. (2009). Interplay between equilibrium and kinetics in prograde metamorphism of pelites: An example from Nelson aureole, British Columbia. *Journal of Metamorphic Geology*, *27*, 249–279. https://doi.org/10.1111/j.1525-1314.2009.00816.x

Phillips, E. R., Key, R. M., Clark, G. C., May, F., Glover, B. W., & Chacksfield, B. C. (1994). Tectonothermal evolution of the Neoproterozoic Grampian and Appin groups, southwestern Monadhliath Mountains, Scotland. *Journal of the Geological Society London*, *151*, 971–986. https://doi.org/10.1144/gsjgs.151.6.0971

Pollok, K., Lloyd, G. E., Austrheim, H., & Putnis, A. (2008). Complex replacement patterns in garnets from Bergen Arcs eclogite: A combined EBSD and analytical TEM study. *Chemie der Erde*, *68*, 177–191. https://doi.org/10.1016/j.chemer.2007.12.002

Putnis, A. (2009). Mineral replacement reactions. *Reviews in Mineralogy and Geochemistry*, *70*, 87–124. https://doi.org/10.2138/rmg.2009.70.3

Putnis, A., & Austrheim, H. (2010). Fluid-induced processes: Metasomatism and metamorphism. *Geofluids*, *10*, 254–269.

Putnis, A., & Putnis, C. V. (2007). The mechanism of reequilibration of solids in the presence of a fluid phase. *Journal of Solid State Chemistry*, *180*, 1783–1786. https://doi.org/10.1016/j.jssc.2007.03.023

Putnis, C. V., Tsukamoto, K., & Nishimura, Y. (2005). Direct observation of pseudomorphism: Compositional and textural evolution at a fluid-solid interface. *American Mineralogist*, *90*, 1909–1912. https://doi.org/10.2138/am.2005.1990

Richardson, S. W., & Powell, R. (1976). Thermal causes of the Dalradian metamorphism in the central Highlands of Scotland. *Scottish Journal of Geology*, *12*, 237–268. https://doi.org/10.1144/sjg12030237

Rubie, D. C. (1986). The catalysis of mineral reactions by water and restrictions on the presence of aqueous fluids during metamorphism. *Mineralogical Magazine*, *50*, 399–415. https://doi.org/10.1180/minmag.1986.050.357.05

Ruiz-Agudo, E., Putnis, C. V., & Putnis, A. (2014). Coupled dissolution and precipitation at mineral-fluid interfaces. *Chemical Geology*, *383*, 132–146. https://doi.org/10.1016/j.chemgeo.2014.06.007

Spear, F. S. (1988). Metamorphic fractional crystallization and internal metasomatism by diffusional homogenization of zoned garnets.

Contributions to Mineralogy and Petrology, *99*, 507–517. https://doi.org/10.1007/BF00371941

Spear, F. S. (1993). *Metamorphic phase equilibria and pressure – temperature – time paths*. Washington, DC: Mineralogical Society of America, 799 pp.

Spear, F. S. (2014). The duration of near-peak metamorphism from diffusion modeling of garnet zoning. *Journal of Metamorphic Geology*, *32*, 903–914. https://doi.org/10.1111/jmg.12099

Spear, F. S., & Cheney, J. T. (1989). A petrogenetic grid for pelitic schists in the system SiO_2-Al_2O_3-FeO-MgO-K_2O-H_2O. *Contributions to Mineralogy and Petrology*, *101*, 149–164. https://doi.org/10.1007/BF00375302

Spear, F. S., Kohn, M. J., Florence, F. P., & Menard, T. (1990). A model for garnet and plagioclase growth in pelitic schists: Implications for thermobarometry and P-T path determinations. *Journal of Metamorphic Geology*, *8*, 683–696. https://doi.org/10.1111/j.1525-1314.1990.tb00495.x

Spear, F. S., & Wolfe, O. M. (2018). Evaluation of the effective bulk rock composition (EBC) during growth of garnet. *Chemical Geology*, *491*, 39–47. https://doi.org/10.1016/j.chemgeo.2018.05.019

Thompson, A. B. (1976). Mineral reactions in pelitic rocks. 1. Prediction of P-T-X (Fe-Mg) relations. *American Journal of Science*, *276*, 401–424. https://doi.org/10.2475/ajs.276.4.401

Thompson, A. B., Tracy, R. J., Lyttle, P. T., & Thompson, J. B. Jr (1977). Prograde reaction histories deduced from compositional zonation and mineral inclusions in garnet from the Gassetts Schist, Vermont. *American Journal of Science*, *277*, 1152–1167. https://doi.org/10.2475/ajs.277.9.1152

Tinkham, D. K., & Ghent, E. H. (2005). Estimating P-T conditions of garnet growth with isochemical phase-diagram sections and the problem of effective bulk-composition. *The Canadian Mineralogist*, *43*, 35–50. https://doi.org/10.2113/gscanmin.43.1.35

Tracy, R. J., Robinson, P., & Thompson, A. B. (1976). Garnet composition and zoning in the determination of temperature and pressure of metamorphism, central Massachusetts. *American Mineralogist*, *61*, 762–775.

Tuccillo, M. E., Essene, E. J., & van der Pluijm, B. A. (1990). Growth and retrograde zoning in garnets from high-grade metapelites: Implications for pressure-temperature paths. *Geology*, *18*, 839–842. https://doi.org/10.1130/0091-7613(1990)018<0839:GARZIG>2.3.CO;2

Vance, D., & Mahar, E. (1998). Pressure-temperature paths from pseudosections and zoned garnets: Potential, limitations and examples from the Zanskar Himalaya, NW India. *Contributions to Mineralogy and Petrology*, *132*, 225–245. https://doi.org/10.1007/s004100050419

Viete, D. R., Hermann, J., Lister, G. S., & Stenhouse, I. R. (2011). The nature and origin of the Barrovian metamorphism, Scotland: Diffusion length scales in garnet and inferred thermal time scales. *Journal of the Geological Society, London*, *168*, 133–146. https://doi.org/10.1144/0016-76492009-164

Waters, D. J., & Lovegrove, D. P. (2002). Assessing the extent of disequilibrium and overstepping of prograde metamorphic reactions in metapelites from the Bushveld Complex aureole, South Africa. *Journal of Metamorphic Geology*, *20*, 135–149. https://doi.org/10.1046/j.0263-4929.2001.00350.x

Wei, C. J., Powell, R., & Clarke, G. L. (2004). Calculated phase equilibria for low- and medium-pressure metapelites in the KFMASH and KMnFMASH systems. *Journal of Metamorphic Geology*, *22*, 495–508. https://doi.org/10.1111/j.1525-1314.2004.00530.x

Whitney, D. L. (1996). Garnets as open systems during regional metamorphism. *Geology*, *24*, 147–150. https://doi.org/10.1130/0091-7613(1996)024<0147:GAOSDR>2.3.CO;2

Whitney, D. L., Cooke, M. L., & Du Frane, A. (2000). Modeling of radial microcracks at corners of inclusions in garnet using fracture mechanics. *Journal of Geophysical Research*, *105*, 2843–2853. https://doi.org/10.1029/1999JB900375

Whitney, D. L., & Evans, B. W. (2010). Abbreviations for names of rock-forming minerals. *American Mineralogist*, *95*, 185–187. https://doi.org/10.2138/am.2010.3371

Whitney, D. L., Mechum, T. A., Dilek, Y., & Kuehner, S. M. (1996). Modification of garnet by fluid infiltration during regional metamorphism in garnet through sillimanite-zone rocks, Duchess County, New York. *American Mineralogist*, *81*, 696–705. https://doi.org/10.2138/am-1996-5-617

Yang, P., & Rivers, T. (2001). Chromium and manganese zoning in pelitic garnet and kyanite: Spiral, overprint, and oscillatory (?) zoning patterns and the role of growth rate. *Journal of Metamorphic Geology*, *19*, 455–474. https://doi.org/10.1046/j.0263-4929.2001.00323.x

Yardley, B. W. D. (1977a). An empirical study of diffusion in garnet. *American Mineralogist*, *62*, 793–800.

Yardley, B. W. D. (1977b). The nature and significance of the mechanism of sillimanite growth in Connemara Schists, Ireland. *Contributions to Mineralogy and Petrology*, *65*, 53–58. https://doi.org/10.1007/BF00373570

Zuluaga, C. A., Stowell, H. H., & Tinkham, D. K. (2005). The effect of zoned garnet on metapelite pseudosection topology and calculated metamorphic P-T paths. *American Mineralogist*, *90*, 1619–1626. https://doi.org/10.2138/am.2005.1741

How to cite this article: Dempster TJ, Gilmour MI, Chung P. The partial equilibration of garnet porphyroblasts in pelitic schists and its control on prograde metamorphism, Glen Roy, Scotland. *J Metamorph Geol*. 2019;37:383–399. https://doi.org/10.1111/jmg.12467